Antibacterial Evaluation of Lithium-Loaded Nanofibrous Poly(L-Lactic Acid) Membranes Fabricated via an Electrospinning Strategy

Chaoan Liang[1†], Qiming Jiang[1†], Yi Yu[1], Tao Xu[2], Hanyu Sun[1], Feilong Deng[1*] and Xiaolin Yu[1*]

[1] Guangdong Provincial Key Laboratory of Stomatology, Department of Oral Implantology, Hospital of Stomatology, Guanghua School of Stomatology, Sun Yat-sen University, Guangzhou, China, [2] Biomanufacturing and Rapid Forming Technology Key Laboratory of Beijing, Key Laboratory for Advanced Materials Processing Technology, Ministry of Education, Department of Mechanical Engineering, Tsinghua University, Beijing, China

Lithium (Li) reportedly has anti-bacterial properties. Thus, it is an ideal option to modify barrier membranes used for guided bone regeneration to inhibit the bacterial adhesion. The aims of this study were to fabricate and characterize nanofibrous poly(L-lactic acid) (PLLA) membranes containing Li, and investigate their antibacterial effects on *Porphyromonas gingivalis* and *Actinobacillus actinomycetemcomitans in vitro*. Li (5%Li, 10%Li, and 15%Li)-loaded nanofibrous PLLA membranes were fabricated using an electrospinning technique, and characterized via scanning electron microscopy, X-ray photoelectron spectroscopy, X-ray diffraction, a contact angle measuring device, and a universal testing machine. Sustained release of Li ions was measured over a 14-day period and biocompatibility of the Li-PLLA membranes was investigated. Evaluation of bacterial adhesion and antibacterial activity were conducted by bacterial colony counting, LIVE/DEAD staining and inhibition zone method using *P.gingivalis* and *A.actinomycetemcomitans*. Of the three Li-loaded membranes assessed, the 10%Li-PLLA membrane had the best mechanical properties and biocompatibility. Adhesion of both *P.gingivalis* and *A.actinomycetemcomitans* on Li-PLLA membranes was significantly lower than adhesion on pure PLLA membranes, particularly with regard to the 10%Li and 15%Li membranes. Significant antibacterial activity of Li-PLLA were also observed against according to the inhibition zone test. Given their better mechanical properties, biocompatibility, and antibacterial activity, PLLAs with 10%Li are a better choice for future clinical utilization. The pronounced antibacterial effects of Li-loaded PLLA membranes sets the stage for further application in guided bone regeneration.

Keywords: anti-bacterial, barrier membranes, lithium, electrospinning, nanofibers

INTRODUCTION

Dental implant therapy is a good choice for patients with partial or complete edentulism. Patients benefit from evolving clinical concepts and strategies by way of better treatment and improved quality of life. One such strategy is guided bone regeneration (GBR) for localized alveolar defects, a technique that uses barrier membranes to prevent epithelial cells and fibroblasts from growing into defects, while ensuring the growth of osteoblasts and blood vessels (Nyman, 1991; Hammerle and Jung, 2003). Numerous animal experiments (Dahlin et al., 1989; Lee et al., 2020) and human clinical studies (Buser et al., 1990; Wachtel et al., 1991; Lang et al., 1994) indicate that GBR is a successful method for augmenting bone in defected areas. Notably, however, postoperative complications can occur due to the complexity of the oral environment. In a recent meta-analysis the incidence of soft tissue complications after GBR procedures was 16.8% (Lim et al., 2018), including membrane exposure, soft tissue dehiscence, and acute infection/abscess. *Porphyromonas gingivalis* (*P.g*) and *Actinobacillus actinomycetemcomitans* (*A.a*) are reportedly the main pathogens that contribute to such infections and inflammation (Kornman and Robertson, 2000) which hinder the process of bone regeneration (Simion et al., 1994). Thus, GBR membranes with antibacterial properties are needed to promote better prognoses.
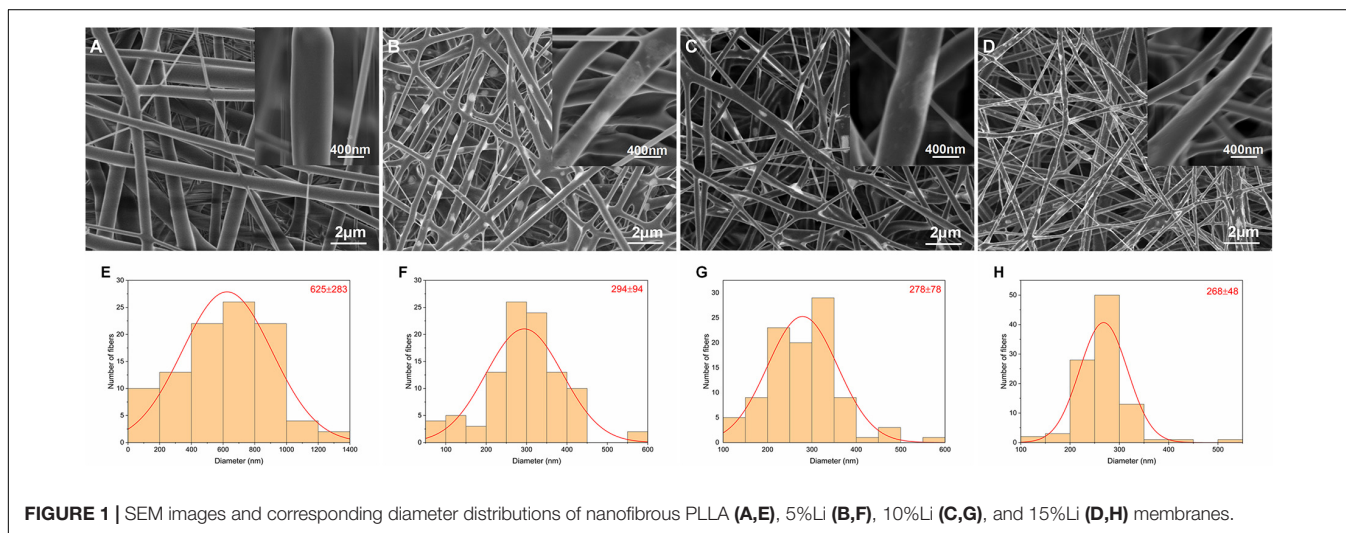
Lithium (Li) is a well-known treatment for bipolar and other psychiatric disorders (Oruch et al., 2014). It is a microelement needed in minute quantities to maintain bodily functions including metabolism, neural communication, and cell proliferation (Schrauzer, 2002; Shahzad et al., 2017) but few studies have investigated the antibacterial and immunopotentiating properties of Li (Shenkman et al., 1980; Zhang et al., 2009; Kalinowska et al., 2011; Tay et al., 2012; Moghanian et al., 2018). In the recent study, Li was substituted for calcium in bioactive glass and reported antibacterial effects *in vitro* (Moghanian et al., 2018). Antibacterial effects of Li in mice infected with *Francisella tularensis* (Zhang et al., 2009)

and *Burkholderia pseudomallei* (Tay et al., 2012) were also, respectively, reported. Thus Li may be an antibacterial substance, but its effects on *P.g* and *A.a* have not been reported.

Recent studies have shown that Li can induce bone formation and osseointegration via the canonical Wnt/β-catenin signaling pathway (Huang et al., 2019). It has also been reported that Li can inhibit the process of osteoclastogenesis (Arioka et al., 2014) and the formation of multinuclear cells in long-term human marrow cultures (Pepersack et al., 1994). Li is therefore a therapeutic option for bone regeneration due to multiple properties.

To obtain GBR membranes for bone regeneration with desirable properties such as biocompatibility, biodegradability, osteoconductivity, osteoinductivity, and antibacterial capacity, electrospinning and related techniques utilizing synthetic and/or natural polymers have attracted increasing interest (Bottino et al., 2012; Shahriar et al., 2019). Electrospinning is a relatively simple and unique method for fabricating nanofibrous membranes (Rodriguez-Tobias et al., 2019). The nanofibers used have a high surface area-to-volume ratio, a controllable degradation rate, favorable mechanical properties, and high porosity. Various materials have been used to generate electrospun fibrous membranes, including poly(L-lactic acid) (PLLA) which has been approved by the Food and Drug Administration for human clinical use due to its outstanding biocompatibility and biodegradability. Wang et al. (2017) developed conductive nanofibrous sheets based on polylactide and polyaniline via electrospinning and indicated their great potential in cardiac tissue engineering and bioactuators applications. Shi et al. (2016) also developed biodegradable PLLA patches with a 3D network structure and reported positive results when they were used for dural repair.

The electrospinning technique was deemed suitable for fabricating the antibacterial membranes used in the current study, and PLLA eventually degrades and creates an acidic environment that may inhibit bacterial growth (Zilberman and Elsner, 2008). In the present study, Li-loaded nanofibrous PLLA membranes were fabricated via electrospinning techniques. The

FIGURE 1 | SEM images and corresponding diameter distributions of nanofibrous PLLA **(A,E)**, 5%Li **(B,F)**, 10%Li **(C,G)**, and 15%Li **(D,H)** membranes.

aim of the study was to characterize these membranes and investigate their antibacterial effects on *P.g* and *A.a in vitro*.

MATERIALS AND METHODS

## Composite Material and Membrane Preparation

Reagents were obtained from Aladdin (China) unless otherwise stated. PLLA (PURAC Biochem, Netherlands) was first dissolved in a mixture of hexafluoroisopropanol and N,N-dimethylformamide (4/1, v/v) at a concentration of 6% w/v, into which Li chloride was added. Li chloride concentrations of 5, 10, and 15% tested. The mixtures were stirred at room temperature. A total of four groups were included in the study; PLLA-only (PLLA), 5% LiCl (5%Li), 10% LiCl (10%Li), and 15% LiCl (15%Li).

Each polymer solution was loaded into a 10-mL syringe. The electrospinning setup consisted of a high-voltage power supply and a digitally controlled syringe pump. The electrospun nanofibrous membranes were collected on an aluminum foil roller. During the process of electrospinning, the distance between the tip of the syringe and the collector was set at 20 cm, and the rotation speed of the roller was set at 100 rpm. The flow rate of the solution was set at 0.2 mL/h, and the applied voltages were set at a range of 15–20 kV. The fibers were deposited layer by layer as a fleece-like structure. The membranes were cut into disks with a diameter of 1 cm.

Characterization of the Nanofibrous PLLA Membranes

Membrane Morphology

The electrospun nanofibrous PLLA and Li-PLLA membranes were coated with gold and their morphologies were assessed

FIGURE 2 | XPS spectra of 5%Li, 10%Li, and 15%Li membranes.
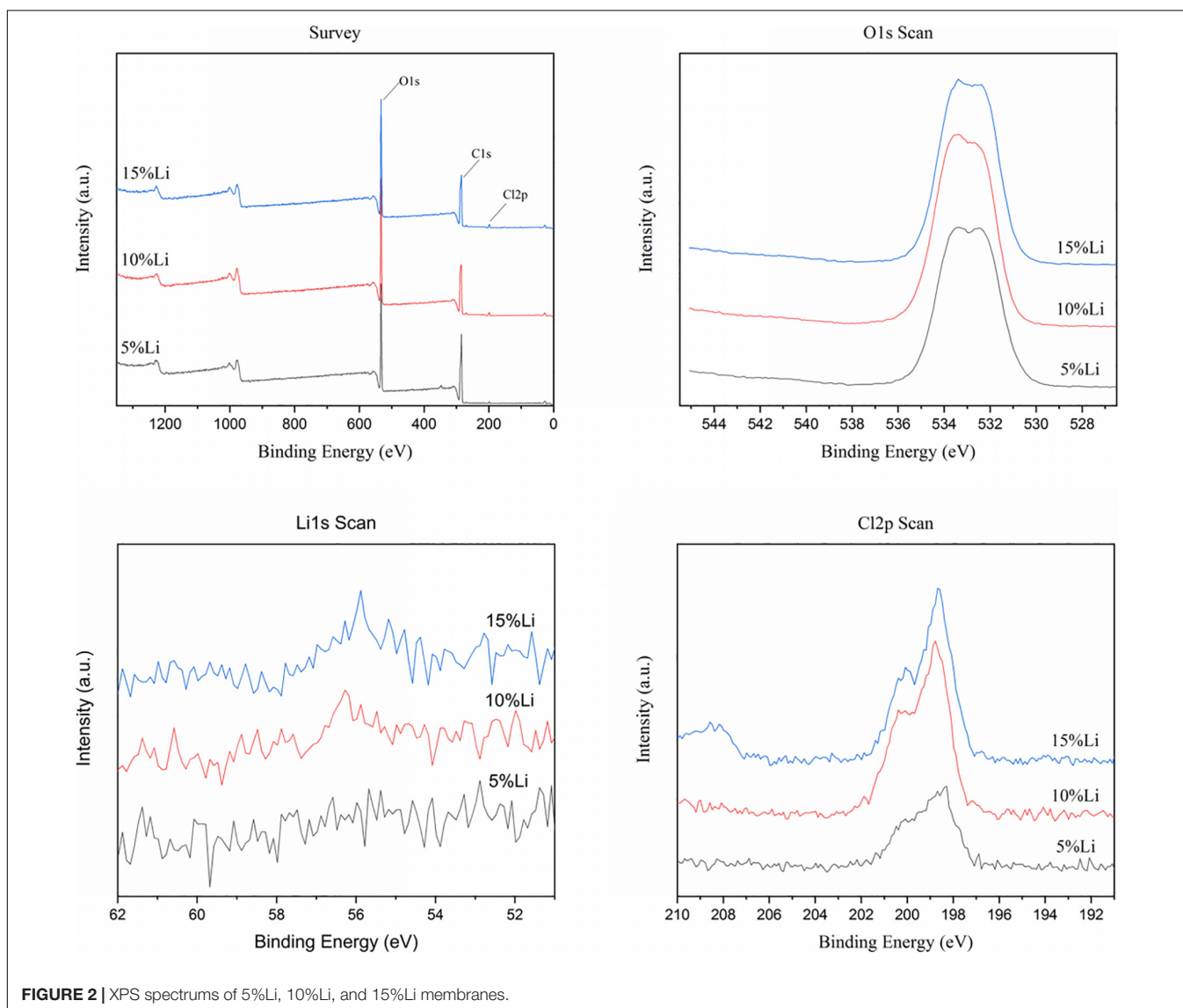
via field-emission scanning electron microscopy (SEM) (S-4800, Hitachi, Tokyo, Japan) at 2 kV. Image-Pro Plus (Rockville, MD, United States) was used to measure fiber diameters and distributions quantitatively.

Elemental Compositions and Phase Analysis of Membranes

Chemical elements were assessed via X-ray photoelectron spectroscopy (XPS) (Thermo Scientific ESCALAB 250Xi, United States). X-ray diffraction (XRD) (X'Pert-PRO, PANalytical, Netherlands) patterns were obtained over a 2θ range of 5°–70° at 40 kV and 40 mA (Cu Kα).

Tensile Strength

The effects of Li incorporation on mechanical membrane performance were tested by evaluating tensile strength with a universal testing machine (Instron 5967, United States). Samples of membrane with a thickness of 0.1 mm were cut into 5 × 20-mm rectangular strips and tested under a constant upper clamp speed of 10 mm/min. Three samples were tested in each group and their tensile strengths were analyzed. The elastic modulus was calculated from the slope of the linear region (ε = 1–4%) of the tensile-stress curve.

Contact Angles

The contact angles of the nanofibrous membranes were measured via the sessile-drop method with an optical contact angle measuring device (OCA40 Micro, Dataphysics, Stuttgart, Germany).

Ion Release From Nanofibrous Li-PLLA Membranes

Li ion release from the samples was determined by assessing changes in ion concentration in pH 7.4 phosphate-buffered saline (PBS) at various timepoints. Samples of 5%Li, 10%Li, and 15%Li were added to PBS at 37°C for 14 days. The PBS was changed every day, and the cumulative ion concentrations at each timepoint were assessed via inductively coupled plasma optical emission spectroscopy (ICP-OES) (Optima 8000DV, Perkin Elmer, United States).

Cell Viability Assay

MC3T3-E1 cells were seeded onto samples in 48-well plates at a density of 1.5×10^4 cells·mL^{-1} and cultured in α-MEM for 1, 4, and 7 days. At each timepoint the Cell Counting Kit-8 assay (CCK-8) (Dojindo, Kumamoto, Japan) was used to assess cell proliferation. One hundred microliters of 10% CCK-8 fluid with medium was added to each well, then the cells were incubated for 2 h. The optical absorbance of the CCK-8 fluid was then measured at 450 nm.

In vitro Bacterial Adhesion and Antibacterial Activity

Bacterial Culture and Adhesion

P.g (ATCC 33277) and *A.a* (ATCC 43717) were used in bacterial adhesion assays. *P.g* was inoculated on brain heart infusion (BHI) agar plates containing sheep blood and vitamin K1. *A.a* was inoculated on BHI agar plates. After incubation under anaerobic conditions at 37°C for 72 h, single colonies of *P.g* and *A.a* were, respectively, transferred to 15-mL centrifuge tubes containing
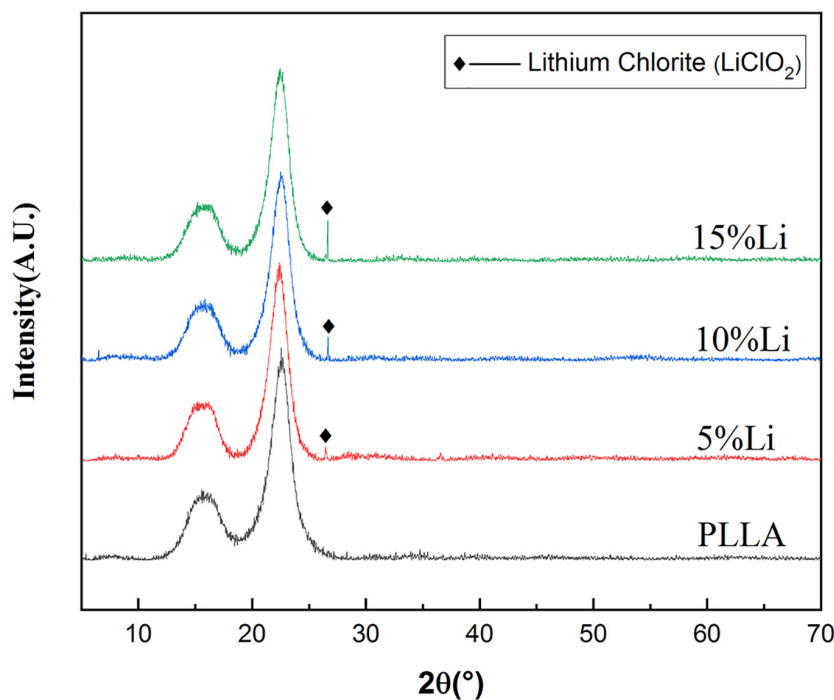

FIGURE 3 | XRD spectrums of PLLA, 5%Li, 10%Li, and 15%Li membranes.

10 mL medium. After incubation under anaerobic conditions at 37°C for another 72 h, the bacterial suspensions were diluted to approximately 1×10^7 colony forming units (CFU)/mL for bacterial adhesion assays and antibacterial activity assessment using the McFarland Scale.

All samples were placed in 48-well non-tissue culture plates and 1 mL of diluted bacterial suspension was added to each sample. After incubation under anaerobic conditions at 37°C for 72 h the samples were rinsed with PBS twice to remove unbound bacteria, and bacterial colony counting and LIVE/DEAD staining assays were conducted using these samples.

To visualize bacterial adherence in the samples, after a 72-h incubation one sample from each group was immersed in 2.5% glutaraldehyde for 10 h at 4°C then subjected to gradient dehydration using 50, 75, 90, 95, and 100% ethanol. After spraying with gold, the samples were observed via SEM.
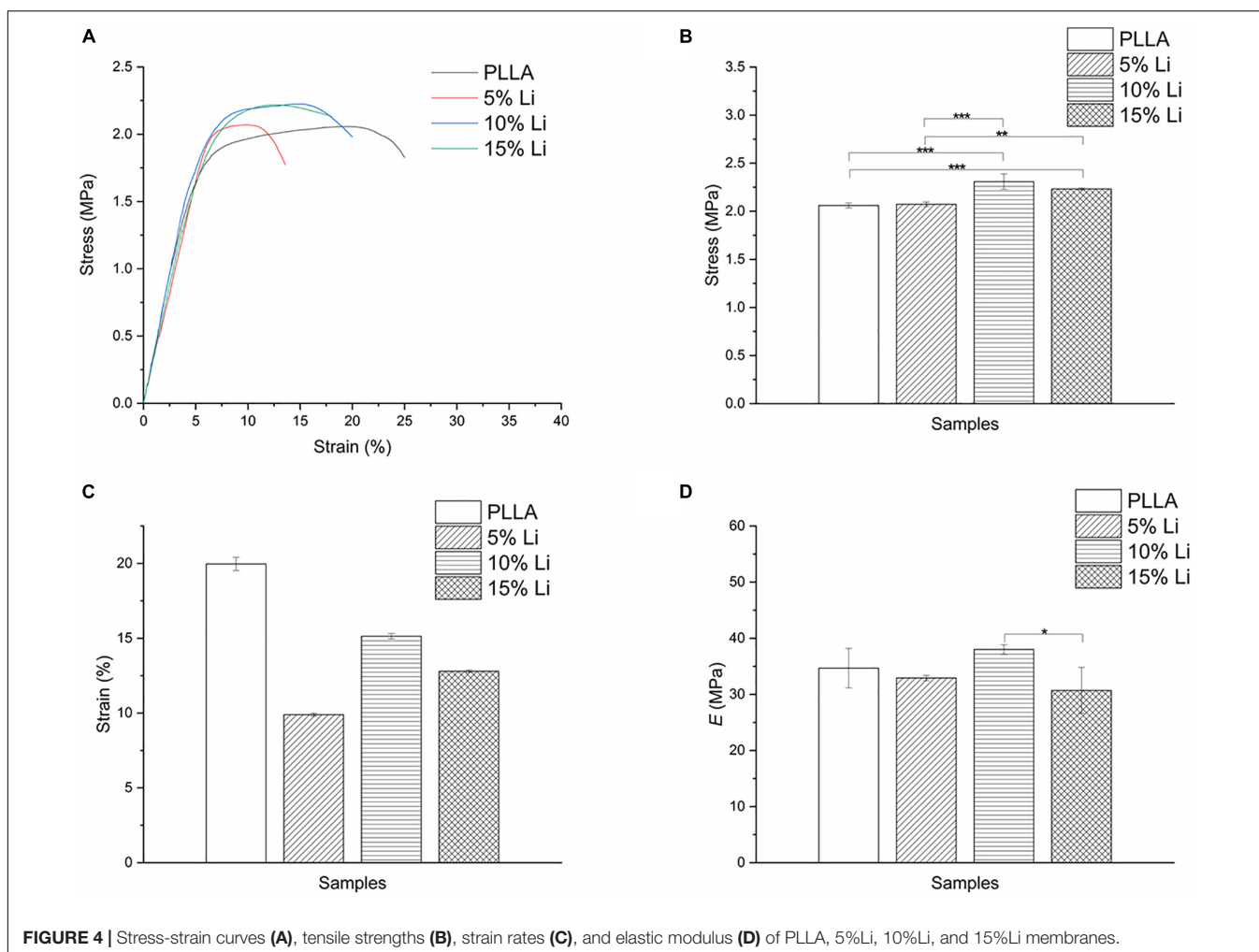
Bacterial Colony Counting

After incubation, the samples were rinsed with PBS then transferred into Eppendorf tubes containing 3 mL PBS. The tubes were sonicated for 5 min, followed by a 15-s vortex to detach adhered bacteria. The treated solutions were then diluted

to suitable concentrations and 100 µL was inoculated onto BHI agar plates. After incubation under anaerobic conditions at 37°C for 72 h, colonies of *P.g* and *A.a* were counted to evaluate the amounts of live adhered bacteria in the samples.

Bacterial LIVE/DEAD Staining

The LIVE/DEAD® BacLight™ Bacterial Viability Kit (L7012, Thermo Scientific, United States) was used to distinguish live and dead bacteria. After incubation the samples were rinsed with PBS then incubated with 200 µL LIVE/DEAD® BacLight™ solution prepared in accordance with the manufacturer's instructions at room temperature in the dark for 15 min. The SYTO 9 in the solution causes the live bacteria to emit green fluorescence, and the propidium iodide in the solution causes dead bacteria to emit red fluorescence. Confocal laser scanning microscopy (CLSM) (Nikon A1 plus, Japan) was used to assess the samples. Image-Pro Plus was used to perform quantitative analysis to evaluate bacterial adhesion based on the determination of fluorescence intensity in each captured image. Results were obtained from three captured images and normalized to the green/total fluorescence intensity of PLLA samples and red fluorescence intensity of 15%Li samples.

FIGURE 4 | Stress-strain curves **(A)**, tensile strengths **(B)**, strain rates **(C)**, and elastic modulus **(D)** of PLLA, 5%Li, 10%Li, and 15%Li membranes.

Assessment of Antibacterial Activity

The inhibition zone method was used for gaging the antibacterial activity of samples (Zhang et al., 2019). One hundred microliters diluted bacterial suspension (1×10^7 CFU/mL) of was uniformly spread across the BHI agar plates, followed by placing sterilized samples onto them. After incubation under anaerobic conditions at 37°C for 72 h, the presence of inhibition zones were recorded and the diameters of them were measured. The experiment was repeated three times.

Statistical Analysis

Statistical analysis was performed using SPSS software, version 23.0 (IBM SPSS, United States). The level of significance was determined by one-way analysis of variance followed by Fisher's least significant difference test for multiple comparisons. The significance level was set at $p < 0.05$.

RESULTS

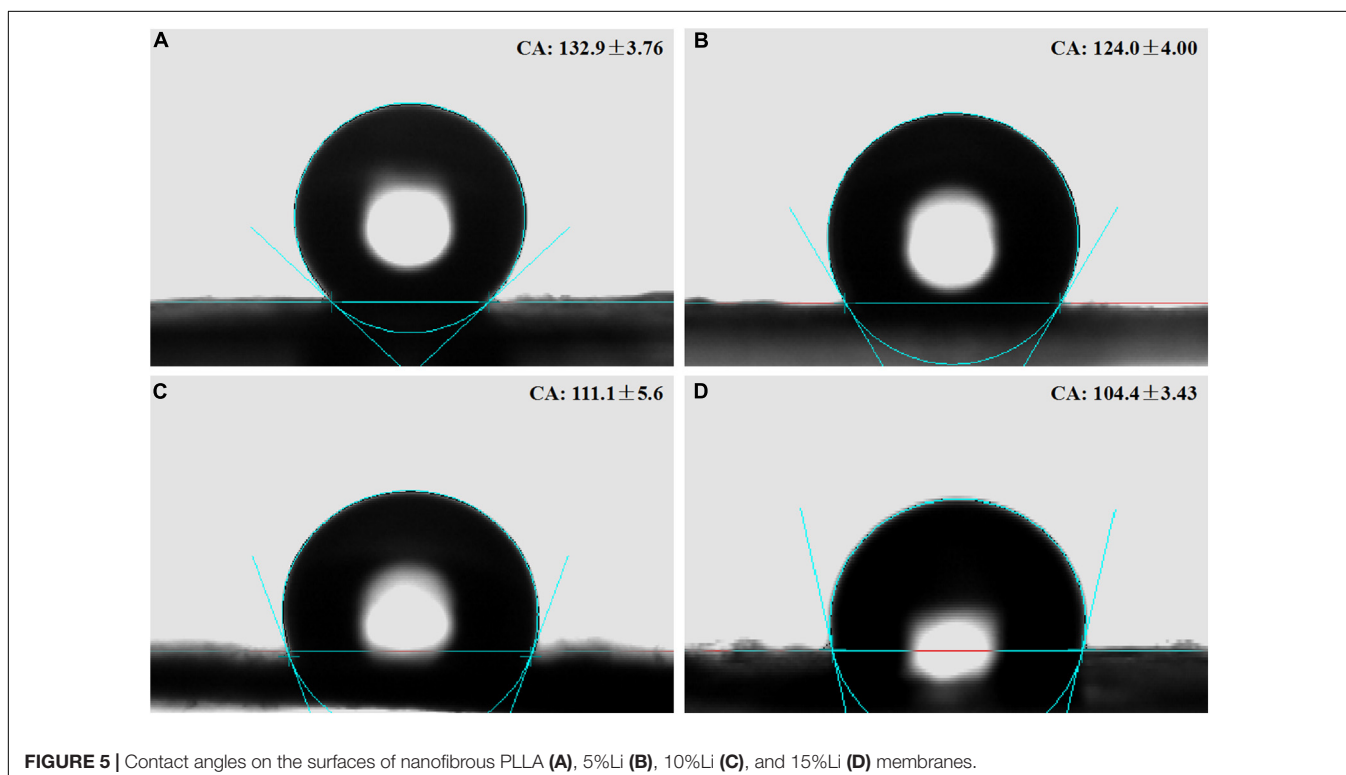## Membrane Characterization

Membrane Morphology

The morphologies and corresponding fiber diameter distributions in the four groups are shown in **Figure 1**. Fibers exhibited a randomly oriented morphology and 3D network structure. Li was visible as white patches in the fibers. The mean fiber diameter tended to decrease with increasing incorporation of Li. This was due to reduced solution viscosity and increased solution conductivity.

Elemental Composition and Phase Analysis

The chemical element compositions of 5%Li, 10%Li, and 15%Li membranes were analyzed via XPS, and the results are shown in **Figure 2**. All three Li-loaded membranes yielded two peaks at approximately 200.1 and 198.6 eV in the Cl 2p spectra, indicating the presence of Cl^{3+} and Cl^+, and a peak at approximately 533.5 eV in the O 1s spectra indicating the presence of O^{2-}. Peaks at approximately 56.0 eV in the Li 1s spectra of 10%Li and 15%Li membranes indicated the presence of Li^+. No Li peak was evident in the Li 1s spectrum of the 5%Li membrane, possibly because the Li content was too low. The diffraction patterns of PLLA membranes with different Li content are shown in **Figure 3**. The XRD spectra of 5%Li, 10%Li, and 15%Li samples exhibited approximate diffraction peaks at approximately 26.5°, corresponding with the lithium chlorite ($LiClO_2$) phase, which was concordant with the XPS results. Other diffraction peaks reflected the presence of PLLA polymer.

Mechanical Properties of the Membranes

Stress-strain curves, maximum tensile strengths, strain rates, and elastic modulus are shown in **Figures 4A–D**. The PLLA and 5%Li membranes exhibited lower tensile strength than the 10%Li and 15%Li membranes ($p < 0.01$), and the PLLA membrane exhibited a superior strain rate. This revealed that the incorporation of Li improved the mechanical strength of the membranes. The 10%Li membrane had a higher elastic modulus than the 15%Li membrane, and a higher strain rate than the 5%Li and 15%Li membranes.

FIGURE 5 | Contact angles on the surfaces of nanofibrous PLLA **(A)**, 5%Li **(B)**, 10%Li **(C)**, and 15%Li **(D)** membranes.

Contact Angle of the Membranes

Water contact angles of the membranes were PLLA 132.9° ± 3.76°, 5%Li 124.0° ± 4.00°, 10%Li 111.1° ± 5.62°, and 15%Li 104.4° ± 3.43° (**Figure 5** and **Table 1**). The results indicated that the incorporation of Li improved the hydrophilicity of nanofibrous PLLA membranes ($p < 0.05$).

Ion Release

Inductively coupled plasma optical emission spectroscopy indicated cumulative release of up to 0.92 mg·L^{-1} Li$^+$ from 5%Li membranes, 1.15 mg·L^{-1} Li$^+$ from 10%Li membranes, and 1.26 mg·L^{-1} Li$^+$ from 15%Li membranes by day 14 (**Figure 6**). An initial burst of release was evident, followed by sustained release. The release rates of 10%Li and 15%Li membranes were more stable than those of 5%Li membranes, at approximately 0.04 mg·L^{-1} per day.

Cell Viability Evaluation

The results of the cell viability assay in each group are shown in **Figure 7**. No toxic effect but pro-proliferative effect was observed at any of the samples. On the 1st day the PLLA and 15%Li groups exhibited more proliferation than the 5%Li and 10%Li groups ($p < 0.05$). On the 4th and 7th days, however, the 10%Li group exhibited more proliferation than any other groups ($p < 0.001$). There were no significant differences between PLLA and 5%Li, PLLA and 15%Li, or 5%Li and 15%Li after 7 days.

In vitro Bacterial Adhesion and Antibacterial Activity

Bacterial Adhesion

The results of bacterial adhesion on the membrane surfaces in each group are shown in **Figure 8**. Representative morphologies of *P.g* and *A.a* were assessed via SEM and there were less bacteria adhering to the 10%Li and 15%Li membranes than to the 5%Li and PLLA membranes. *P.g* tended to form a biofilm on PLLA membranes, whereas a filamentous structure was observed around and between *A.a* on PLLA membranes.

Bacterial Colony Counting

The results of bacterial colony counting assays are shown in **Figure 9**. After a 72-h incubation there were significantly more *P.g* and *A.a* CFU on PLLA membranes than on any of the three Li-loaded membranes. There was no statistically significant difference between the *A.a* CFU on 5%Li and 10%Li membranes, or the *P.g* CFU on 10%Li and 15%Li membranes.
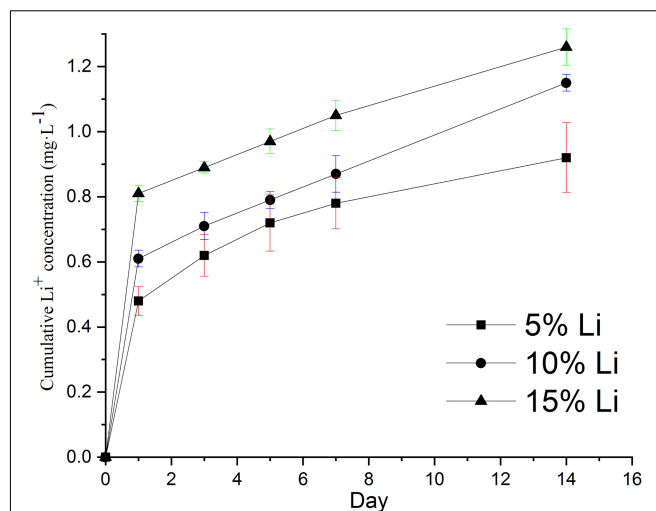

FIGURE 6 | *In vitro* cumulative release concentrations of Li ions from 5%Li, 10%Li, and 15%Li membranes after incubation in PBS at 37°C for 14 d. Data are expressed as means ± the standard deviation ($n = 3$).
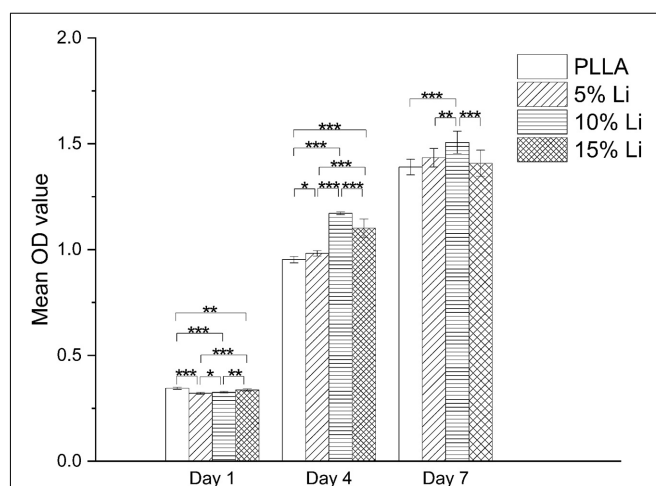

FIGURE 7 | MC3T3-E1 cell proliferation on the surfaces of each membrane after 1, 4, and 7 days. Data are expressed as means ± the standard deviation ($n = 3$). *$p < 0.05$, **$p < 0.01$, ***$p < 0.001$.

Bacterial LIVE/DEAD Staining

Adherence of *P.g* and *A.a* after 72 h were assessed via CLSM after LIVE/DEAD staining, and there were differences in the ratios of live/dead bacteria on the surfaces of each sample (**Figures 10**, **11**). Viable *P.g* and *A.a* occupied almost every fiber on the surface of PLLA membranes. Results of quantitative analysis are shown in **Figure 12**. Increased Li content was associated with significantly lower numbers of viable bacteria and significantly higher numbers of dead bacteria. These results were consistent with the results of the bacterial colony counting assays. Thus, Li-loading had antibacterial effects against *P.g* and *A.a*.
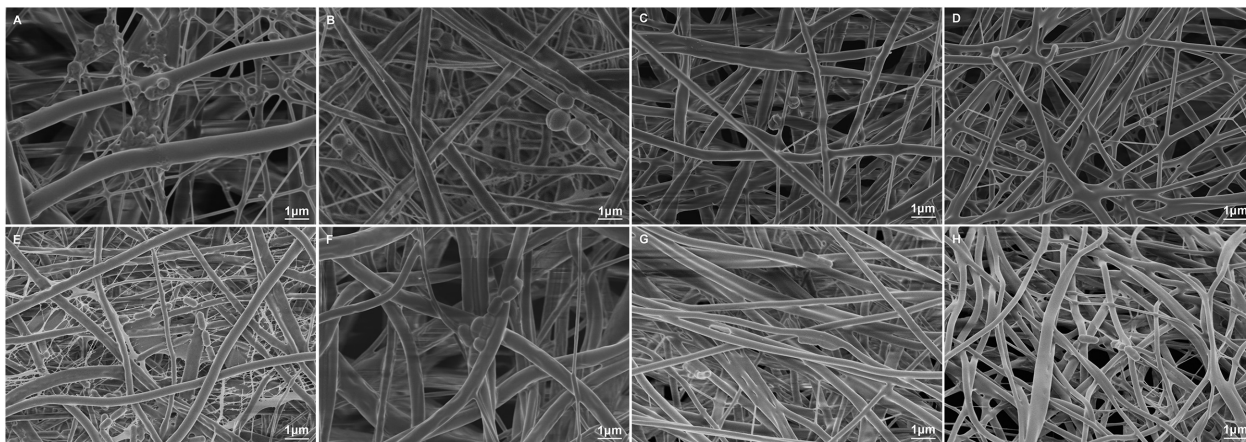
TABLE 1 | Water contact angles of the samples.

	Contact angle (°)	*p*-value		
		PLLA	5%Li	10%
PLLA	132.9 ± 3.76	–	–	–
5%Li	124.0 ± 4.00	0.034	–	
10%Li	111.1 ± 5.62	0.000	0.006	–
15%Li	104.4 ± 3.43	0.000	0.001	0.092

FIGURE 8 | Representative SEM images of *P.g* adhesion on the surfaces of PLLA **(A)**, 5%Li **(B)**, 10%Li **(C)**, and 15%Li **(D)** membranes, and *A.a* adhesion on the surfaces of PLLA **(E)**, 5%Li **(F)**, 10%Li **(G)**, and 15%Li **(H)** membranes after incubation for 72 h.
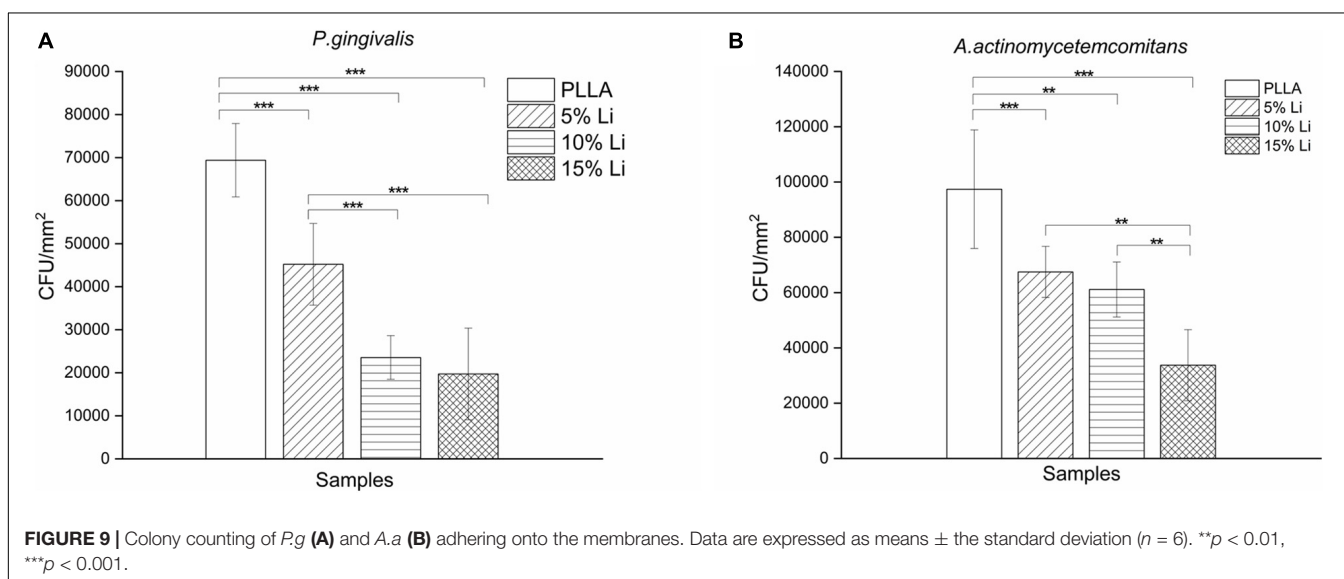

FIGURE 9 | Colony counting of *P.g* **(A)** and *A.a* **(B)** adhering onto the membranes. Data are expressed as means ± the standard deviation (n = 6). **$p < 0.01$, ***$p < 0.001$.

Assessment of Antibacterial Activity

The antibacterial activity of the Li-loaded nanofibers was evaluated based on disk diffusion against *P.g* and *A.a*, as shown in **Figure 13A**. Inhibition zone was observed around 5%Li, 10%Li, and 15%Li, confirming the growth inhibition of *P.g* and *A.a*. The diameters of inhibition zone were measured in millimeters and presented in **Figure 13B**.

DISCUSSION

Membranes used in GBR are expected to have multiple functions such as inducing proliferation/differentiation of osteoblasts while inhibiting that of osteoclasts, and antibacterial properties. Several reports indicate that Li that can promote bone formation (Zamani et al., 2009; Chen and Alman, 2009; Cai et al., 2015; Zhang et al., 2018), and a few (Tay et al., 2012; Moghanian et al., 2018) imply that it has antibacterial potential, thus

it may be suitable for improving membrane properties. To our knowledge, Li has not been incorporated into electrospun membranes before. In the current study, Li-loaded nanofibrous PLLA membranes with a 3D network structure were generated via an electrospinning technique. Li was successfully electrospun into the fibers, which subsequently exhibited Li ion release. The Li-loaded membranes also exhibited good biocompatibility and antibacterial properties against *P.g* and *A.a*.

Based on the electrospinning technique, Bartnikowski et al. (2018) fabricated a 3D printed polycaprolactone scaffold with Li incorporated into it and reported delayed leaching and immunomodulatory effects of bioactive ions. In the present study, parameters such as solution viscosity, Li concentration, and flow rate were manipulated to generate stable nanofibrous membranes with uniformly distributed Li. Under SEM, Li was visualized as white patches or spots, similar to other metals (Jin et al., 2018; Rajzer et al., 2019) when loaded into fibers. The diameter distribution also suggested that the
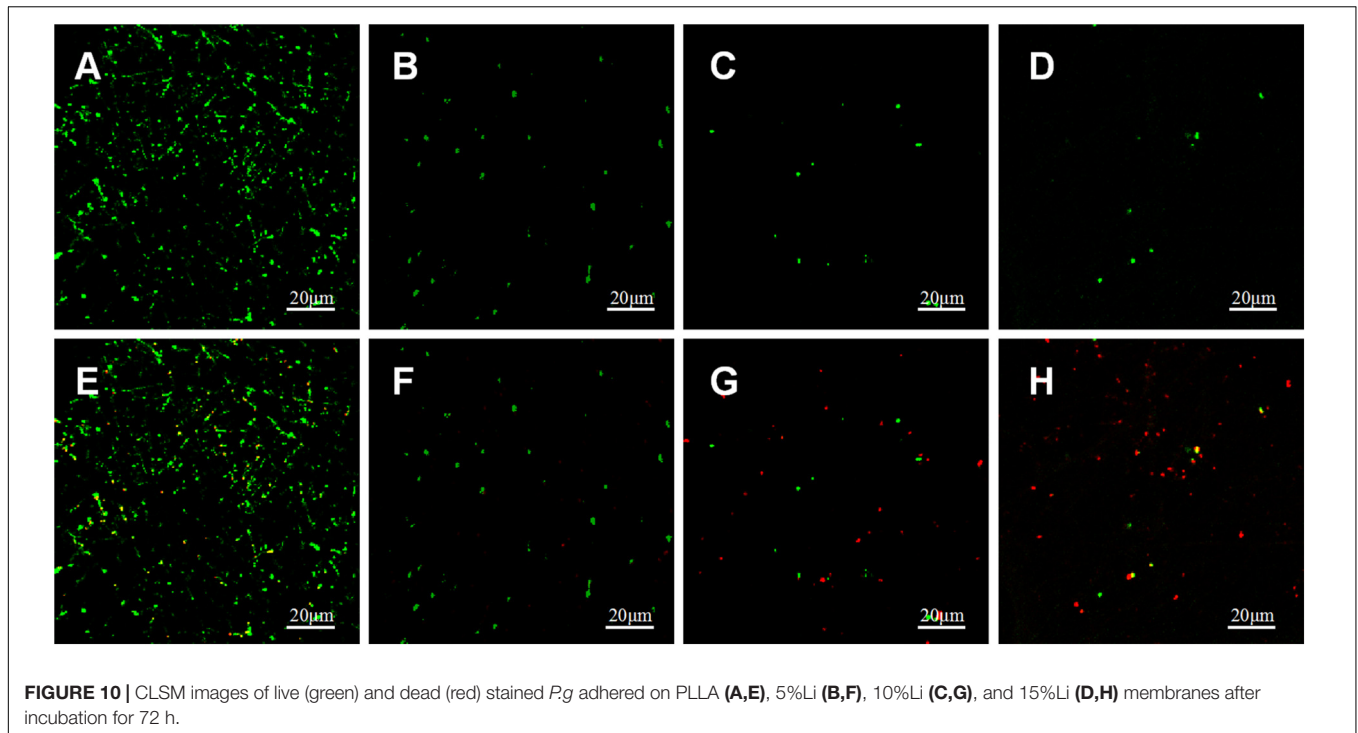
FIGURE 10 | CLSM images of live (green) and dead (red) stained *P.g* adhered on PLLA **(A,E)**, 5%Li **(B,F)**, 10%Li **(C,G)**, and 15%Li **(D,H)** membranes after incubation for 72 h.
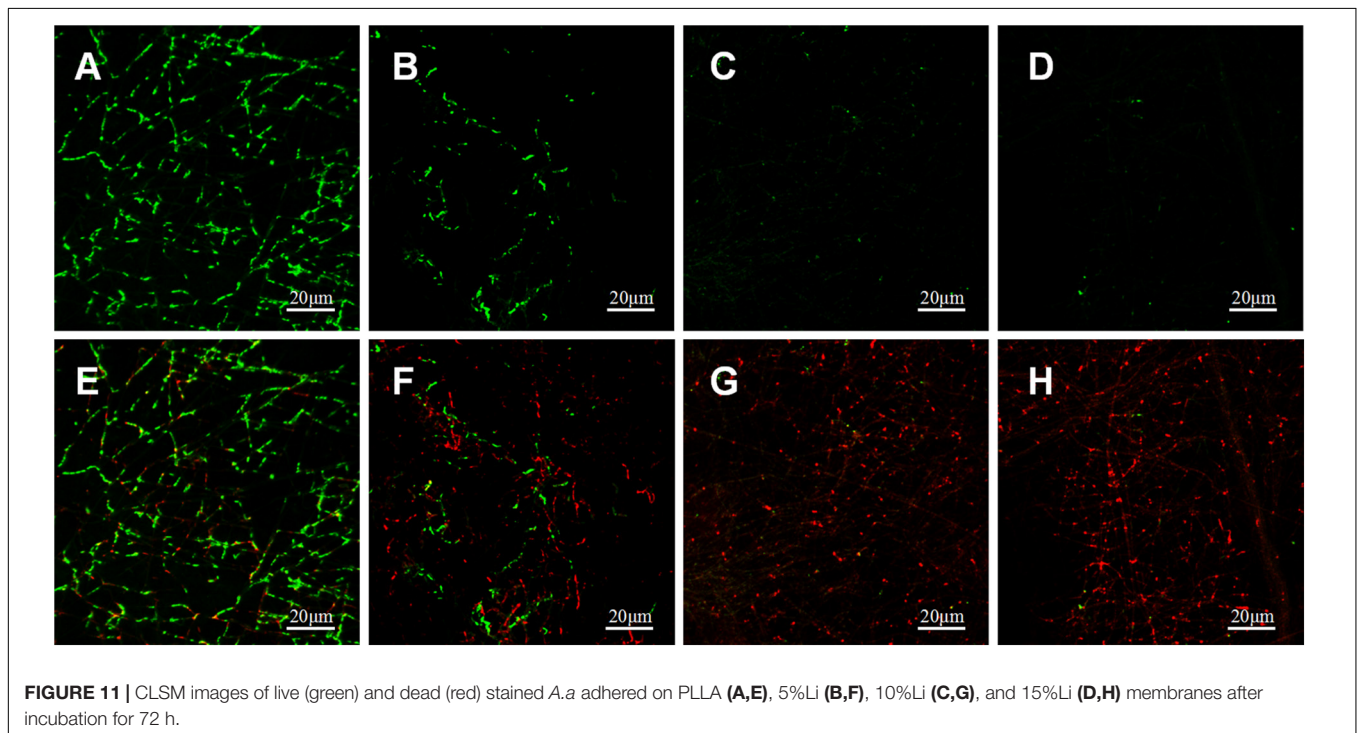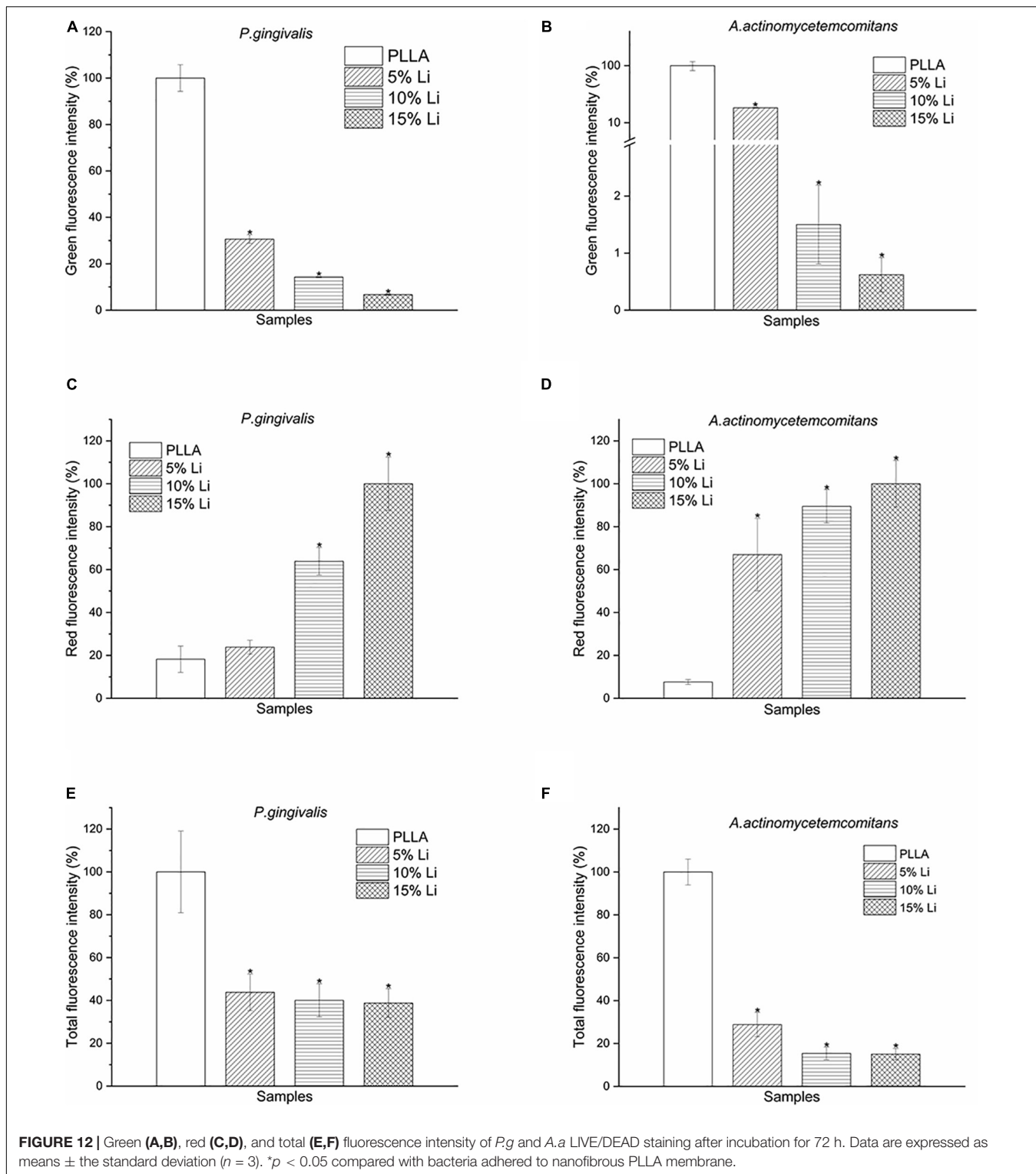

FIGURE 11 | CLSM images of live (green) and dead (red) stained *A.a* adhered on PLLA **(A,E)**, 5%Li **(B,F)**, 10%Li **(C,G)**, and 15%Li **(D,H)** membranes after incubation for 72 h.
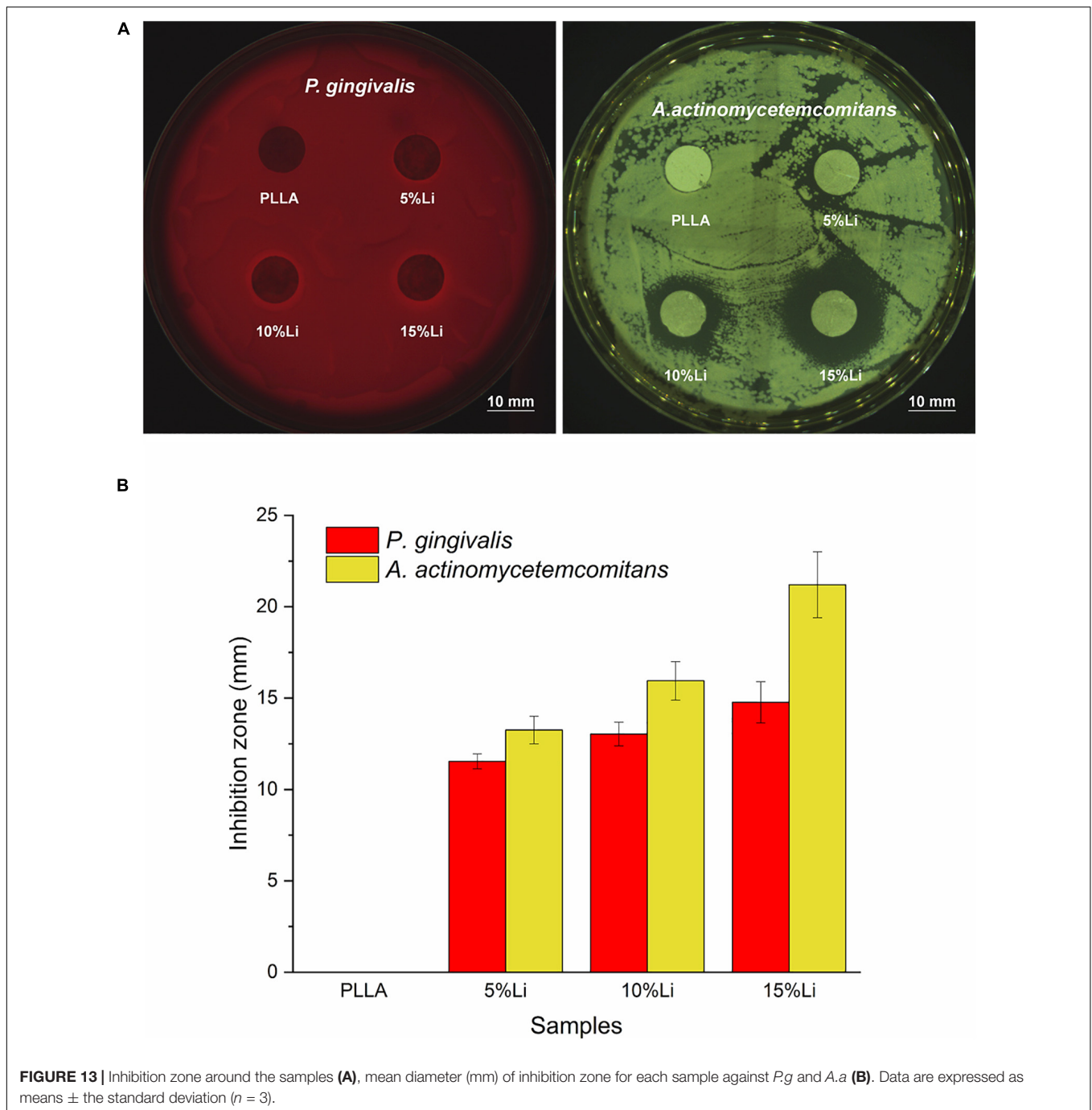
addition of Li may assist the fabrication of finer fibers with improved mechanical properties (Kidoaki et al., 2006). To prove this, we evaluated the mechanical properties of each group via tensile tests. 10%Li and 15%Li exhibited higher maximum tensile strengths, indicating that the addition of Li enhanced the mechanical strength of the membranes. 10%Li

had a higher elastic modulus than 15%Li, suggesting better properties in this regard. We believe that the reason for the higher elastic modulus of 10%Li is related to the stability of facbricating process. An increased Li concentration may result in excessively higher conductivity and lower viscosity of the solution, leading to unstable fabrication and droplet formation

FIGURE 12 | Green **(A,B)**, red **(C,D)**, and total **(E,F)** fluorescence intensity of *P.g* and *A.a* LIVE/DEAD staining after incubation for 72 h. Data are expressed as means ± the standard deviation (*n* = 3). *p < 0.05 compared with bacteria adhered to nanofibrous PLLA membrane.

on the membranes (Kidoaki et al., 2006; Stachewicz et al., 2012). More Li will be accumulated in the droplets and less will be incorporated into the fibers, resulting in a non-uniform distribution. In the present study, 15%Li resulted in a relatively stable electrospinning process, indicating that that concentration

of Li was in the appropriate range. However, comparing to 10%Li, 15%Li probably caused less uniform distribution of Li, resulting in less elastic modulus. In a previous study, fibers with smaller diameters had higher strength but lower ductility (Stachewicz et al., 2012), and similar results were observed in the

FIGURE 13 | Inhibition zone around the samples **(A)**, mean diameter (mm) of inhibition zone for each sample against *P.g* and *A.a* **(B)**. Data are expressed as means ± the standard deviation (*n* = 3).

current study in which the PLLA membrane exhibited a superior strain rate. The 10%Li membrane exhibited greater ductility than the 5%Li and 15%Li membranes, further illustrating the advantages of 10%Li.

The hydrophilicity of the nanofibrous membranes was improved by Li incorporation. The contact angle of the membranes decreased with increasing incorporation of Li. The improved hydrophilicity meets the requirement of barrier membranes, but notably a higher Li content is not necessarily better as mentioned above.

The results of cumulative Li release were as expected. At the early stage there was an initial burst of release, which may assist the avoidance of bacterial contamination during the first 6 h after GBR (Hetrick and Schoenfisch, 2006). Subsequent sustained Li release from the membranes over 14 d has the potential to further prevent bacterial colonization. In the current study the cumulative Li concentration was always within the safe limit (Shahzad et al., 2017; Medic et al., 2020), namely 1.2 mM for humans. This and the results of the CCK-8 assays attest to the biological safety of 3D printed Li-loaded nanofibrous

membranes. The results of CCK-8 assays also revealed that the incorporation of Li had a tendency to promote MC3T3-E1 cell proliferation, which is concordant with previous studies (Clement-Lacroix et al., 2005; Liu et al., 2018), implying the medical potential of the membranes. The capacity of the 10%Li membranes to promote cell proliferation was greatest at the 7-day timepoint, again demonstrating the importance of the appropriate Li concentration. Notably, however, the *in vivo* biological safety and pro-proliferative effects of Li-loaded membranes require further study.

Prevention of pathogenic bacterial adhesion can reduce the occurrence of infection and promote a stable prognosis after surgery. One purpose of the current study was to evaluate the antibacterial effects of nanofibrous Li-PLLA membranes. The hydrophilicity of a material's surface is one of the factors that affects bacterial adhesion. Generally, hydrophilic surfaces have higher surface free energy and attract more bacteria with high surface free energy. Early in 1995, Quirynen and Bollen (1995) investigated the influence of tooth surface on supragingival and subgingival plaque formation, and concluded that increased surface free energy resulted in faster colonization and maturation of plaque. In the present study the improved hydrophilicity and surface free energy of the nanofibrous membranes may have increased the adherence of bacteria. Bacterial colony counting and LIVE/DEAD staining conducted with *P.g* and *A.a* revealed that there was less bacterial adhesion on Li-PLLA membranes than on PLLA membranes, however, confirming the antibacterial activity of the incorporated Li. For *P.g*, 10%Li and 15%Li had similar antibacterial effects and they were superior to those of 5%Li. For *A.a*, 5%Li and 10%Li had similar effects and they were inferior to those of 15%Li. In addition, the antibacterial activity against *P.g* and *A.a* was also verified by the appearance of inhibition zone. The diameter of inhibition zone increased with the increasing concentration of Li. Generally, the size of inhibition zone related to the susceptibility of bacteria to the test agent. Our results suggested that A.a is more susceptible to Li. Taking biocompatibility into consideration, 10%Li is a better choice for future improvement and clinical utilization. Nevertheless, the optimum concentration of Li should be further investigated, particularly between 10 and 15%.

The exact mechanisms of the effects of Li are not yet clear. In CLSM experiments, membranes with greater Li content exhibited less viable bacteria and more dead bacteria on their surfaces than pure PLLA membranes. This suggests that Li has bactericidal effects or inhibits bacteria adhesion. Moghanian et al. (2018) reported similar results with Li-substituted bioactive glass. Studies (Tallon et al., 2007) have shown that Li may affect proteins involved in adhesion, whose physiochemical properties such as hydrophobicity are related to adhesion. Another possibility is that Li cations induce electrotransformation of bacteria and increase the permeability of cell membranes (Papagianni et al., 2007; Ramon and Fonzi, 2009) causing the accumulation of Li + in the cell cytoplasm and inhibition of pyruvate kinase (Niiya et al., 1980; Umeda et al., 1984). Li ions may also influence ion channels or replace other cations, affecting bacterial membranes. The exact mechanism should be further studied *in vivo* because Li is also associated with immunomodulatory effects.

In the present study, the incorporation of Li had antibacterial effects on *P.g* and *A.a.* It has previously been reported that Li rendered bacteria more sensitive to acid (Gallagher and Cutress, 1977). In the current study PLLA was used as the basic material, and it ultimately degrades and creates an acidic environment, promoting the reduction of bacterial aggregation. The use of Li as a treatment for bone regeneration has been extensively studied, but its antibacterial properties in this context have not. Hence, further confirmation of the antibacterial effects of Li-loaded nanofibrous PLLA membranes and their effects on bone regeneration are required to establish its viability as a barrier membrane for GBR.

CONCLUSION

In the present study, Li-loaded nanofibrous PLLA membranes were generated via an electrospinning technique. They exhibited a 3D network structure, sustained release of Li ions, improved mechanical strength, and hydrophilicity. The Li-loaded PLLA fibers significantly reduced the adherence and inhibited the growth of *P.g* and *A.a* compared to PLLA fibers alone, particularly the 10%Li and 15%Li membranes. Given their better mechanical properties and biocompatibility, 10%Li is a high-potential multifunctional candidate in the field of GBR.

DATA AVAILABILITY STATEMENT

The raw data supporting the conclusions of this article will be made available by the authors, without undue reservation.

AUTHOR CONTRIBUTIONS

FUNDING

ACKNOWLEDGMENTS

REFERENCES

Arioka, M., Takahashi-Yanaga, F., Sasaki, M., Yoshihara, T., Morimoto, S., Hirata, M., et al. (2014). Acceleration of bone regeneration by local application of lithium: Wnt signal-mediated osteoblastogenesis and Wnt signal-independent suppression of osteoclastogenesis. *Biochem. Pharmacol.* 90, 397–405. doi: 10.1016/j.bcp.2014.06.011

Bartnikowski, M., Moon, H. J., and Ivanovski, S. (2018). Release of lithium from 3D printed polycaprolactone scaffolds regulates macrophage and osteoclast response. *Biomed. Mater.* 13:065003. doi: 10.1088/1748-605X/aad916

Bottino, M. C., Thomas, V., Schmidt, G., Vohra, Y. K., Chu, T. M., Kowolik, M. J., et al. (2012). Recent advances in the development of GTR/GBR membranes for periodontal regeneration–a materials perspective. *Dental Mater.* 28, 703–721. doi: 10.1016/j.dental.2012.04.022

Buser, D., Bragger, U., Lang, N. P., and Nyman, S. (1990). Regeneration and enlargement of jaw bone using guided tissue regeneration. *Clin. Oral Implants Res.* 1, 22–32. doi: 10.1034/j.1600-0501.1990.010104.x

Cai, Y., Guo, L., Shen, H., An, X., Jiang, H., Ji, F., et al. (2015). Degradability, bioactivity, and osteogenesis of biocomposite scaffolds of lithium-containing mesoporous bioglass and mPEG-PLGA-b-PLL copolymer. *Int. J. Nanomed.* 10, 4125–4136. doi: 10.2147/IJN.S82945

Chen, Y., and Alman, B. A. (2009). Wnt pathway, an essential role in bone regeneration. *J. Cell. Biochem.* 106, 353–362. doi: 10.1002/jcb.22020

Clement-Lacroix, P., Ai, M., Morvan, F., Roman-Roman, S., Vayssiere, B., Belleville, C., et al. (2005). Lrp5-independent activation of Wnt signaling by lithium chloride increases bone formation and bone mass in mice. *Proc. Natl. Acad. Sci. U S A.* 102, 17406–17411. doi: 10.1073/pnas.0505259102

Dahlin, C., Sennerby, L., Lekholm, U., Linde, A., and Nyman, S. (1989). Generation of new bone around titanium implants using a membrane technique: an experimental study in rabbits. *Int. J. Oral Maxillofacial Implants* 4, 19–25.

Gallagher, I. H., and Cutress, T. W. (1977). The effect of trace elements on the growth and fermantation by oral streptococci and actinomyces. *Arch. Oral Biol.* 22, 555–562. doi: 10.1016/0003-9969(77)90066-8

Hammerle, C. H., and Jung, R. E. (2003). Bone augmentation by means of barrier membranes. *Periodontology* 2000, 36–53. doi: 10.1046/j.0906-6713.2003.03304.x

Hetrick, E. M., and Schoenfisch, M. H. (2006). Reducing implant-related infections: active release strategies. *Chem. Soc. Rev.* 35, 780–789. doi: 10.1039/b515219b

Huang, T. B., Li, Y. Z., Yu, K., Yu, Z., Wang, Y., Jiang, Z. W., et al. (2019). Effect of the Wnt signal-RANKL/OPG axis on the enhanced osteogenic integration of a lithium incorporated surface. *Biomater. Sci.* 7, 1101–1116. doi: 10.1039/c8bm01411f

Jin, S., Li, J., Wang, J., Jiang, J., Zuo, Y., Li, Y., et al. (2018). Electrospun silver ion-loaded calcium phosphate/chitosan antibacterial composite fibrous membranes for guided bone regeneration. *Int. J. Nanomed.* 13, 4591–4605. doi: 10.2147/IJN.S167793

Kalinowska, M., Piekut, J., and Lewandowski, W. (2011). Relationship between chemical structure and biological activity of alkali metal o-, m- and p-anisates. FT-IR and microbiological studies. *Spectrochimica Acta Part A: Mol. Biomol. Spectroscopy* 82, 432–436. doi: 10.1016/j.saa.2011.07.074

Kidoaki, S., Kwon, I. K., and Matsuda, T. (2006). Structural features and mechanical properties of in situ-bonded meshes of segmented polyurethane electrospun from mixed solvents. *J. Biomed. Mater. Res. Part B Appl. Biomater.* 76, 219–229. doi: 10.1002/jbm.b.30336

Kornman, K. S., and Robertson, P. B. (2000). Fundamental principles affecting the outcomes of therapy for osseous lesions. *Periodontology* 22, 22–43. doi: 10.1034/j.1600-0757.2000.2220103.x

Lang, N. P., Hammerle, C. H., Bragger, U., Lehmann, B., and Nyman, S. R. (1994). Guided tissue regeneration in jawbone defects prior to implant placement. *Clin. Oral Implants Res.* 5, 92–97. doi: 10.1034/j.1600-0501.1994.050205.x

Lee, J., Lee, Y. M., Lim, Y. J., and Kim, B. (2020). Ridge augmentation using beta-tricalcium phosphate and biphasic calcium phosphate sphere with collagen membrane in chronic pathogenic extraction sockets with dehiscence defect: a pilot study in beagle dogs. *Materials (Basel)* 13:1452. doi: 10.3390/ma13061452

Lim, G., Lin, G. H., Monje, A., Chan, H. L., and Wang, H. L. (2018). Wound healing complications following guided bone regeneration for ridge augmentation: a systematic review and meta-analysis. *Int. J. Oral Maxillofacial Implants* 33, 41–50. doi: 10.11607/jomi.5581

Liu, W., Chen, D., Jiang, G., Li, Q., Wang, Q., Cheng, M., et al. (2018). A lithium-containing nanoporous coating on entangled titanium scaffold can enhance osseointegration through Wnt/beta-catenin pathway. *Nanomedicine* 14, 153–164. doi: 10.1016/j.nano.2017.09.006

Medic, B., Stojanovic, M., Stimec, B. V., Divac, N., Vujovic, K. S., Stojanovic, R., et al. (2020). Lithium - pharmacological and toxicological aspects: the current state of the Art. *Curr. Med. Chem.* 27, 337–351. doi: 10.2174/0929867325666180904124733

Moghanian, A., Firoozi, S., Tahriri, M., and Sedghi, A. (2018). A comparative study on the in vitro formation of hydroxyapatite, cytotoxicity and antibacterial activity of 58S bioactive glass substituted by Li and Sr. *Mater. Sci. Eng. C-Materials Biol. Appl.* 91, 349–360. doi: 10.1016/j.msec.2018.05.058

Niiya, S., Moriyama, Y., Futai, M., and Tsuchiya, T. (1980). Cation coupling to melibiose transport in *Salmonella typhimurium*. *J. Bacteriol.* 144, 192–199. doi: 10.1128/JB.144.1.192-199.1980

Nyman, S. (1991). Bone regeneration using the principle of guided tissue regeneration. *J. Clin. Periodontol.* 18, 494–498. doi: 10.1111/j.1600-051x.1991.tb02322.x

Oruch, R., Elderbi, M. A., Khattab, H. A., Pryme, I. F., and Lund, A. (2014). Lithium: a review of pharmacology, clinical uses, and toxicity. *Eur. J. Pharmacol.* 740, 464–473. doi: 10.1016/j.ejphar.2014.06.042

Papagianni, M., Avramidis, N., and Filioussis, G. (2007). High efficiency electrotransformation of *Lactococcus lactis* spp. lactis cells pretreated with lithium acetate and dithiothreitol. *BMC Biotechnol.* 7:15. doi: 10.1186/1472-6750-7-15

Pepersack, T., Corazza, F., Demulder, A., Guns, M., Fondu, P., and Bergmann, P. (1994). Lithium inhibits calcitriol-stimulated formation of multinucleated cells in human long-term marrow cultures. *J. Bone Mineral Res.* 9, 645–650. doi: 10.1002/jbmr.5650090509

Quirynen, M., and Bollen, C. M. (1995). The influence of surface roughness and surface-free energy on supra- and subgingival plaque formation in man. a review of the literature. *J. Clin. Periodontol.* 22, 1–14. doi: 10.1111/j.1600-051x.1995.tb01765.x

Rajzer, I., Dziadek, M., Kurowska, A., Cholewa-Kowalska, K., Ziabka, M., Menaszek, E., et al. (2019). Electrospun polycaprolactone membranes with Zn-doped bioglass for nasal tissues treatment. *J. Mater. Sci. - Mater. Med.* 30:80. doi: 10.1007/s10856-019-6280-4

Ramon, A. M., and Fonzi, W. A. (2009). Genetic transformation of *Candida albicans*. *Methods Mol. Biol.* 499, 169–174. doi: 10.1007/978-1-60327-151-6_16

Rodriguez-Tobias, H., Morales, G., and Grande, D. (2019). Comprehensive review on electrospinning techniques as versatile approaches toward antimicrobial biopolymeric composite fibers. *Mater. Sci. Eng. C-Mater. Biol. Appl.* 101, 306–322. doi: 10.1016/j.msec.2019.03.099

Schrauzer, G. N. (2002). Lithium: occurrence, dietary intakes, nutritional essentiality. *J. Am. College Nutrit.* 21, 14–21. doi: 10.1080/07315724.2002.10719188

Shahriar, S., Mondal, J., Hasan, M. N., Revuri, V., Lee, D. Y., and Lee, Y. K. (2019). Electrospinning nanofibers for therapeutics delivery. *Nanomaterials (Basel)* 9:532. doi: 10.3390/nano9040532

Shahzad, B., Mughal, M. N., Tanveer, M., Gupta, D., and Abbas, G. (2017). Is lithium biologically an important or toxic element to living organisms? an overview. *Environ. Sci. Poll. Res. Int.* 24, 103–115. doi: 10.1007/s11356-016-7898-0

Shenkman, L., Borkowsky, W., and Shopsin, B. (1980). Lithium as an immunologic adjuvant. *Med. Hypotheses* 6, 1–6. doi: 10.1016/0306-9877(80)90025-0

Shi, Z., Xu, T., Yuan, Y., Deng, K., Liu, M., Ke, Y., et al. (2016). A new absorbable synthetic substitute with biomimetic design for dural tissue repair. *Art. Organs* 40, 403–413. doi: 10.1111/aor.12568

Simion, M., Baldoni, M., Rossi, P., and Zaffe, D. (1994). A comparative study of the effectiveness of e-PTFE membranes with and without early exposure during the healing period. *Int. J. Period. Restorat. Dentistry* 14, 166–180.

Stachewicz, U., Bailey, R. J., Barber, A. H., and Wang, W. (2012). Size dependent mechanical properties of electrospun polymer fibers from a composite structure. *Poly. Int. J. Sci. Technol. Poly.* 53, 5132–5137. doi: 10.1016/j.polymer.2012.08.064

Tallon, R., Arias, S., Bressollier, P., and Urdaci, M. C. (2007). Strain- and matrix-dependent adhesion of *Lactobacillus plantarum* is mediated by proteinaceous

bacterial compounds. *J. Appl. Microbiol.* 102, 442–451. doi: 10.1111/j.1365-2672.2006.03086.x

Tay, T. F., Maheran, M., Too, S. L., Hasidah, M. S., Ismail, G., and Embi, N. (2012). Glycogen synthase kinase-3beta inhibition improved survivability of mice infected with *Burkholderia pseudomallei. Trop. Biomed.* 29, 551–567.

Umeda, K., Shiota, S., Futai, M., and Tsuchiya, T. (1984). Inhibitory effect of Li+ on cell growth and pyruvate kinase activity of *Escherichia coli. J. Bacteriol.* 160, 812–814. doi: 10.1128/JB.160.2.812-814.1984

Wachtel, H. C., Langford, A., Bernimoulin, J. P., and Reichart, P. (1991). Guided bone regeneration next to osseointegrated implants in humans. *Int. J. Oral Maxillofacial Implants* 6, 127–135.

Wang, L., Wu, Y., Hu, T., Guo, B., and Ma, P. X. (2017). Electrospun conductive nanofibrous scaffolds for engineering cardiac tissue and 3D bioactuators. *Acta Biomater.* 59, 68–81. doi: 10.1016/j.actbio.2017.06.036

Zamani, A., Omrani, G. R., and Nasab, M. M. (2009). Lithium's effect on bone mineral density. *Bone* 44, 331–334. doi: 10.1016/j.bone.2008.10.001

Zhang, J., Cai, L., Wang, T., Tang, S., Li, Q., Tang, T., et al. (2018). Lithium doped silica nanospheres/poly(dopamine) composite coating on polyetheretherketone to stimulate cell responses, improve bone formation and osseointegration. *Nanomedicine* 14, 965–976. doi: 10.1016/j.nano.2018.01.017

Zhang, P., Katz, J., and Michalek, S. M. (2009). Glycogen synthase kinase-3beta (GSK3beta) inhibition suppresses the inflammatory response to *Francisella* infection and protects against tularemia in mice. *Mol. Immunol.* 46, 677–687. doi: 10.1016/j.molimm.2008.08.281

Zhang, Q., Wang, Y., Zhang, W., Hickey, M. E., Lin, Z., Tu, Q., et al. (2019). In situ assembly of well-dispersed Ag nanoparticles on the surface of polylactic acid-Au@polydopamine nanofibers for antimicrobial applications. *Colloids Surfaces B: Biointerfaces* 184:110506. doi: 10.1016/j.colsurfb.2019.110506

Zilberman, M., and Elsner, J. J. (2008). Antibiotic-eluting medical devices for various applications. *J. Controll. Release* 130, 202–215. doi: 10.1016/j.jconrel.2008.05.020